Available online at www.sciencedirect.com
ScienceDirect
Catalysis Today 118 (2006) 237–245
CATALYSIS TODAY
www.elsevier.com/locate/cattod

Co-current and counter-current modes for methanol steam reforming membrane reactor: Experimental study

A. Basile [a,*], S. Tosti [b,1], G. Capannelli [c,2], G. Vitulli [d,3], A. Iulianelli [e,4], F. Gallucci [a,5], E. Drioli [a,e,4,5]

[a] *Institute on Membrane Technology, ITM-CNR, c/o University of Calabria, via P. Bucci, Cubo 17/C, 87030 Rende (CS), Italy*
[b] *ENEA, Unità Tecnico Scientifica Fusione, C.R. ENEA Frascati, via E. Fermi 45, Frascati, 00044 Roma, Italy*
[c] *Dipartimento di Chimica e Chimica Industriale, University of Genova, via Dodecaneso 31, 16146 Genova, Italy*
[d] *Istituto di Chimica dei Composti Organometallici, ICCOM-CNR, c/o University of Pisa, via Risorgimento 35, 50126 Pisa, Italy*
[e] *Department of Chemical Engineering and Materials, University of Calabria, via P. Bucci Cubo 42/A, 87030 Rende (CS), Italy*

Available online 7 July 2006

Abstract

The methanol steam reforming (MSR) reaction to produce hydrogen was studied from an experimental point of view in membrane reactors (MRs). In order to investigate the behaviour of methanol conversion, the influence of the membrane characteristics, the sweep gas flow rate, as well as the influence of the operating temperature and the different flux configurations were analysed. Experimental results, in terms of methanol conversion as well as hydrogen production and gases selectivity in MRs and a traditional reactor (TR), are proposed. A set of values of key parameters to obtain the maximum hydrogen production is given.

Keywords: Methanol; Steam reforming; Hydrogen; Catalyst; Membrane reactor; Counter-current mode

1. Introduction

Polymeric fuel-cell systems are electrochemical devices able to generate electrical power by the electrochemical oxidation of hydrogen with atmospheric oxygen. Many studies about hydrogen production for fuel cells deal with the use of two types of carbon compounds: the first type is oxygen-containing compounds, such as methanol, ethanol, while the second one is represented by hydrocarbons, such as natural gas, propane gas, gasoline, etc. [1–8]. The use of methanol as an on-board hydrogen source represents an attractive solution for fuel-cell engines in transportation applications. The advantages of methanol include: easier handling and transportation than gases, low cost, ease of synthesis from a lot of feedstocks (biomass, coal, natural gas, etc.), mild conditions in the reaction. The disadvantages of methanol include the lower energy density, relatively high concentration of CO in the reaction products, which is still much higher than the limit of tolerance of CO concentration in feed gas for polymer electrolyte membrane (PEM) fuel cells. Specifically, for the last case, a CO-free hydrogen stream is necessary for feeding these fuel cells.

Among the different possible reactions involving methanol, the methanol steam reforming (MSR) reaction is viewed as a very interesting and promising method for hydrogen production useful for fuel-cell applications.

This reaction system, when carried out in a traditional system, leads to a hydrogen-containing mixture, so hydrogen needs purification before being fed to a PEM fuel cell. This separation is mainly devoted to removing carbon monoxide, which poisons the anodic catalyst of the fuel cell [9]. For this purpose, a fuel-cell drive system based on methanol as fuel consists of a methanol steam reformer and a gas cleaning unit, which reduces the carbon monoxide content of the

* Corresponding author. Tel.: +39 0984 492013; fax: +39 0984 402103.
E-mail address: a.basile@itm.cnr.it (A. Basile).
[1] Tel.: +39 06 94005160; fax: +39 06 94005374.
[2] Tel.: +39 010 3536197; fax: +39 010 353 8733.
[3] Tel.: +39 050 2219224; fax: +39 050 2219260.
[4] Tel.: +39 0984 492039; fax: +39 0984 402103.
[5] Tel.: +39 0984 492013; fax: +39 0984 402103.

0920-5861/$ – see front matter
doi:10.1016/j.cattod.2006.05.086

hydrogen-rich gas and feeds the fuel cell. The reformer is equipped with a catalytic burner which provides the process heat to the reformer itself and converts all burnable gases of the flue gas into water and carbon dioxide. Recent studies concern the use of MRs for the methanol steam reforming reaction [10–21]. The main advantage is to perform both reaction and pure hydrogen removal in the same device: in this way, it would be possible to replace the traditional system (reformer + gas cleaning unit) with the membrane reactor [9,10]. Furthermore, using steam as a sweep gas for hydrogen removal from the shell side of the membrane reactor, the hydrogen wet stream could be directly suitable for the fuel cell. Actually, compared to methanol and gasoline, among the fuel options for fuel-cell vehicles, liquid hydrogen and compressed hydrogen (up to 34.5 MPa) are predicted to be the most advantageous [17]. However, hydrogen could require unacceptable high infrastructure costs. Vice versa, infrastructure costs for liquid fuels (for example methanol) should be noticeably lower. In this view methanol steam reforming can be seen as fuel source for producing hydrogen in situ at the local fuelling station [17].

In a previous paper [18], from a theoretical viewpoint, a palladium–silver MR was considered with special attention to the hydrogen recovery increase with respect to a TR. After the model validation, the methanol conversion as well as the high hydrogen recovery improvements were observed by changing several reaction parameters: such as time factor, H_2O/CH_3OH feed ratio, reaction temperature, pressure and sweep gas flow rate. In a recent theoretical paper [19], the MR theoretical analysis was extended by considering other two different operative conditions, when shell side and lumen side streams are in co-current mode or in counter-current mode. In another two experimental works [20,21] the methanol steam reforming reaction as well as the oxidative methanol steam reforming reaction were studied in the palladium–silver MR by using a Cu-based catalyst. The operative conditions investigated were the temperature, the H_2O/CH_3OH feed flow rate and the O_2/CH_3OH feed flow rate (for the oxidative methanol steam reforming). The two works showed the potentiality of membrane reactor in terms of methanol conversion as well as hydrogen production with respect to a traditional system.

In the present work, three different membranes were used in the membrane reactor and the co-current and counter-current modes were analysed from an experimental point of view. The aim is to find the best condition to maximize the CO-free hydrogen production.

2. Description of the process

2.1. Traditional and membrane reactors description

The TR consists of a stainless steel tube, length 250 mm, i.d. 6.7 mm, the reaction zone is 150 mm. The MR consists of a tubular stainless steel module [22], length 280 mm, i.d. 20 mm, containing different membranes, the first one (MR1) is a TiO_2–Al_2O_3 asymmetric porous commercial membrane (Inoceramic) with a Pd–Ag deposit. The second membrane (MR2) is an asymmetric porous ceramic membrane with a Pd–Ag deposit. The third membrane (MR3) is a pine-hole free Pd–Ag thin wall membrane tube permeable only to hydrogen having thickness 50 μm, o.d. 10 mm, length 150 mm. In particular, the dense membrane is joined to two stainless steel tube ends useful for the membrane housing. In the MRs, catalyst pellets are packed in the membrane zone (150 mm length) while glass spheres (2 mm diameter) are placed into the supports on both extremities of the membrane.

For the MR1 and the MR2 two graphite o-rings (99.53% C and 0.47% S; 2.8 g each) furnished by Gee Graphite Ltd. (England), ensure that permeate and lumen streams do not mix with each other in the membrane module. For the MR3 just one graphite o-ring is necessary.

The first membrane was produced at the CNR-ICCOM laboratories (Pisa, Italy) by depositing Pd and Ag on the TiO_2–Al_2O_3 asymmetric support. A Pd–mesitylene-1,exene solution (2 mg/ml Pd content) was used to deposit the palladium. The support was treated with two different solution samples with volume of 6 ml in hydrogen environment (1 atm) for 24 h. Afterwards, the Ag was deposited by vacuum evaporation of acetone from an Ag–acetone solution. The deposition was obtained. The membrane obtained (24 mg Pd and 6 mg Ag) was washed with acetone and dried under vacuum.

The second membrane was produced at the University of Genoa laboratories by depositing Pd and Ag on the ceramic asymmetric support. A Pd–Ag/acetone solution (Pd 1.3 mg/l and Ag 0.4 mg/l) is used to create the deposited layer. The deposition was obtained by vaporisation of Pd and Ag with acetone in a multi-electrodes reactor and afterwards vacuum evaporation of acetone. The membrane obtained (13 mg Pd and 4 mg Ag) was washed with acetone and dried under vacuum.

The third membrane was produced by a cold-rolling and diffusion welding technique in ENEA laboratories (Frascati, Italy); details of this technique have been presented elsewhere by Tosti et al. [23,24]. The upper temperature limit of the Pd–Ag membrane is 450 °C. The tubular membrane is plugged from one side and reactants are fed by means of a stainless steel tube (o.d. 1/16 in., i.d. 1/40 in.) placed inside the membrane lumen in a finger-type configuration: in this way, the membrane tube is free in its elongation/contraction due to the hydrogenation cycling and any mechanical stress is avoided allowing a longer life time.

2.2. Pure gases permeation experiments

Permeation experiments with pure gases were performed with each membrane.

Table 1 resumed the permeation test for the MR1. It can be seen that the H_2/other gas selectivity (calculated as $\alpha_{H_2/\text{other gas}} = P_{H_2}/P_{\text{other gas}}$) is between 2 and 4.5. The MR2 presents similar behaviour to the MR1.

The experimental tests on the dense Pd–Ag membrane MR3 show that H_2/other gas selectivity is infinite and that both Sievert and Arrhenius laws are followed. The linear trend

Table 1
Pure gas permeation tests at different temperatures for the MR1

T (°C)	P_{H_2} (mol m/s bar m^2)	α_{H_2/CO_2} (–)	α_{H_2/CH_4} (–)	$\alpha_{H_2/CO}$ (–)	α_{H_2/N_2} (–)
350	0.0199	2.88	2.84	4.52	2.34
400	0.0161	2.33	2.56	4.03	2.30
450	0.0158	2.29	2.72	4.39	2.59
500	0.0137	1.99	2.69	4.15	2.63
550	0.0135	1.99	2.70	4.50	2.60
600	0.0115	2.21	2.61	3.97	2.25

permitted to calculate the main permeation parameters: the apparent activation energy E_a, found to be equal to 33.31 kJ/mol, and a pre-exponential factor Pe_0 of 1.66×10^{-5} mol m/(m^2 s kPa$^{0.5}$). In this way, the temperature dependence of hydrogen permeability can be expressed by the well-known Arrhenius-like expression: $Pe = Pe_0 \exp(-E_a/RT)$. In conclusion, the overall hydrogen permeation flux, J_{H_2} (mol/m^2 s) through the Pd–Ag membrane can be written by using the Richardson equation:

$$J_{H_2} = \frac{Pe_0 \exp(-E_a/RT)\left(\sqrt{p_{H_2,lumen}} - \sqrt{p_{H_2,shell}}\right)}{\delta} = 3.32 \times 10^{-1} \exp\left(-\frac{4006.5}{T}\right) \times \left(\sqrt{p_{H_2,lumen}} - \sqrt{p_{H_2,shell}}\right) \quad (1)$$

where δ (m) is the membrane thickness.

Table 2 shows a comparison among the permeation parameters (E_a and Pe_0) of different literature works. The parameters calculated in this work are coherent with experimental data found in the literature.

2.3. Experimental details

The reactor (TR or MRs) is placed in a temperature-controlled P.I.D. (proportional + integral + derivative control) oven. Reaction and permeation temperatures are in the range between 350 and 600 °C for MR1 and MR2, while the temperature range is 350–450 °C for MR3. The sweep gas (N_2) is fed by means of a mass-flow controller (Brooks Instruments 5850S) driven by a computer software furnished by Lira (Italy) and used for all of the experiments. H_2O and CH_3OH are fed by means of volumetric pumps (type FMQG6) furnished by General Control (Italy).

Table 2
Apparent activation energy and pre-exponential factor from the literature

E_a (kJ/mol)	Pe_0 [10^{-5} mol m/(s m^2 kPa$^{0.5}$)]	Reference
33.31	1.66	This work
48.50	9.33	[23]
29.73	7.71	[25]
15.70	2.19	[26]
15.50	2.54	[27]
18.45	1.02	[28]
12.48	0.38	[29]

The reaction pressure is held up to 1.3 bar by means of a regulating-valve system placed at the outlet side. Considering the MR, permeate pressure is always 1 bar, and N_2 is used as the sweep gas with the flow rate in the range between 0.5 and 12 ml/s. The methanol feed flow rate is 1.278×10^{-4} mol/s while the H_2O/CH_3OH feed ratio is 4.5. This value of feed flow ratio was chosen in order to avoid or to minimize the carbon deposition on the catalyst surface. The same equipment was used for permeation tests. H_2O and CH_3OH liquid reactants are mixed and vaporised, and then are fed in the reactor (both TR and MRs). The outlet streams are completely condensed in order to remove the un-reacted H_2O and CH_3OH, and then the liquid phase is analysed by means of an Abbe Refractometer at 25 °C. The dry gaseous stream flow rate is measured by means of bubble flow-meters; its composition is detected by using a temperature programmed HP 6890 Gas Chromatograph (GC) with a TCD (Thermal Conductivity Detector) at 250 °C and He as carrier gas. The GC is equipped by three packed columns: Porapack R 50/80 (8 ft × 1/8 in.) and Carboxen^{TM} 1000 (15 ft × 1/8 in.) connected in series, Molecular Sieve 5 Å (6 ft × 1/8 in.); a 10-way valve was used to optimise the total time of the analysis, which was about 7 min. This apparatus is driven by a software furnished by Hewlett-Packard. Considering MRs, since they have two outlet streams (permeate and retentate), two TCD detectors were simultaneously used for measuring their composition at the same time.

Both the TR and the MRs were packed with 3 g of a 5 wt% $Ru–Al_2O_3$ commercial catalyst furnished by Johnson Matthey. Before reaction, the catalyst was pre-heated using N_2 at 400 °C under atmospheric pressure and, afterwards, reduced by using H_2 (1.5×10^{-3} mol/min) at the same temperature for 2 h.

A flat temperature profile along the reactor during the reaction has been observed by using a three points thermocouple inserted into the lumen of both the TR and the MRs.

Fig. 1 shows a simple sketch of the membrane reactor. It can be seen that for MR1 and MR2 the shell inlet side is closed because no sweep gas is used (a). For the MR3, that showed the best performances in terms of hydrogen selectivity and reaction conversion, the sweep gas is used in both co-current mode (b) and counter-current mode (c).

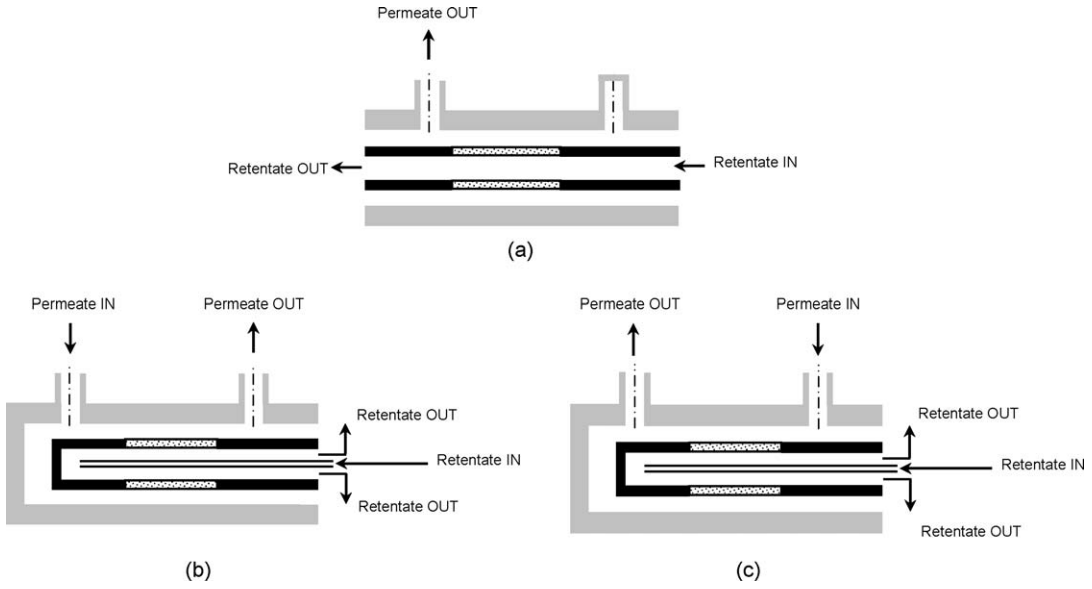

Fig. 1. Scheme of the membrane reactors: (a) for MR1 and MR2, (b) MR3 in co-current mode and (c) MR3 in counter-current mode.

3. Results and discussion

3.1. Definitions

The following definitions are used for describing the TR and the MRs performances:

$$\mathrm{CH_3OH\ conversion}\ (X_{\mathrm{CH_3OH}}, \%) = \frac{\mathrm{CH_3OH_{in}} - \mathrm{CH_3OH_{out}}}{\mathrm{CH_3OH_{in}}} \times 100 \quad (2)$$

$$\mathrm{H_2\ selectivity}\ (S_{\mathrm{H_2}}, \%) = \frac{\mathrm{H_{2,out}}}{\mathrm{H_{2,out}} + \mathrm{CO_{out}} + \mathrm{CO_{2,out}} + \mathrm{CH_{4,out}}} \times 100 \quad (3)$$

$$\mathrm{CO\ selectivity}\ (S_{\mathrm{CO}}, \%) = \frac{\mathrm{CO_{out}}}{\mathrm{H_{2,out}} + \mathrm{CO_{out}} + \mathrm{CO_{2,out}} + \mathrm{CH_{4,out}}} \times 100 \quad (4)$$

$$\mathrm{CO_2\ selectivity}\ (S_{\mathrm{CO_2}}, \%) = \frac{\mathrm{CO_{2,\ out}}}{\mathrm{H_{2,out}} + \mathrm{CO_{out}} + \mathrm{CO_{2,out}} + \mathrm{CH_{4,out}}} \times 100 \quad (5)$$

$$\mathrm{CH_4\ selectivity}\ (S_{\mathrm{CH_4}}, \%) = \frac{\mathrm{CH_{4,out}}}{\mathrm{H_{2,out}} + \mathrm{CO_{out}} + \mathrm{CO_{2,out}} + \mathrm{CH_{4,out}}} \times 100 \quad (6)$$

The subscript ‘‘out’’ indicates the total outlet flow rate of each specie. Specifically, for the TR only one outlet stream is present for each specie, while for the MRs there are two outlet streams. Specifically, in the permeate stream of the MR3 only hydrogen and sweep gas are present, because the dense Pd–Ag membrane exhibits infinite permselectivity H_2/other species. An overall balance on the C-atoms was made for each test and for each membrane. The results confirm that no other C-containing species are present in the mixture and confirm also the results in terms of methanol conversion.

3.2. Comparison between TR and MRs

Fig. 2 reports a comparison, in terms of methanol conversion versus temperature among the TR and the MRs. It should be noted that for the TR the methanol conversion shows a constant trend in the range of temperature investigated; the average value is about 90%. Vice versa, concerning to the membrane reactors, it can be seen that the methanol conversion increases by increasing the temperature for all the three membranes used. In fact, with the MR1, the methanol conversion is about 30% at 350 °C and about 100% at 600 °C while with the MR2 methanol conversion is about 45% at 350 °C and about 65% at 550 °C. Finally, the MR3 shows a methanol conversion 87% at 350 °C and 100% at 450 °C. Specifically, for temperatures

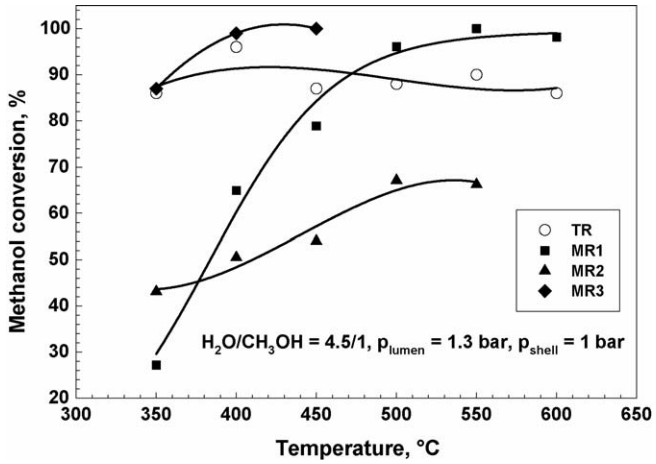

Fig. 2. Methanol conversion vs. temperature for the TR and the MRs, $H_2O/CH_3OH = 4.5/1$, $p_{\mathrm{lumen}} = 1.3$ bar, $p_{\mathrm{shell}} = 1$ bar (for MRs).

lower than 500 °C the TR shows a methanol conversion higher than the MR1, while at temperatures higher than 500 °C the trend is opposite. This fact can be explained by considering that, for low temperatures the reactants permeation rate is higher than the reaction rate, and so a large part of the reactants is lost from the reaction zone and the methanol conversion is lower than that of the TR. At high temperature, the permeation rate is lower than the reaction rate and so the advantage of the products removal gives a methanol conversion higher than the TR. Regarding the MR2, the methanol conversion is always lower than TR and only for $T = 350$ °C the MR2 gives a methanol conversion higher than the MR1. The methanol conversion in MR3 is always higher than the TR with the same temperature.

It can be seen that the advantages in the use of the MRs are evident when only one product (e.g. hydrogen) is removed from the reaction zone, like in the MR3. If also reactants can permeate through the membrane, the operative conditions have to be well-tuned in order to reach methanol conversions higher than the TR (i.e. the reaction rate is bigger than the reactants permeation rate, MR1).

Table 3 reports the results in terms of gases concentration in the shell side and in the lumen side for the MR2. In this case the concentrations in shell side are different from the lumen side ones, but the different concentrations do not give better results in terms of methanol conversion and this is because of the high loss of methanol and water from the reaction zone. For this reactor, the CO content in the shell side can still poison the anodic catalyst of a fuel cell.

Fig. 3 shows the selectivity for the products in the MR1. It can be noted that the hydrogen selectivity is almost constant in all the range of temperature considered and the value is almost 70%. The carbon monoxide selectivity decreases by increasing the temperature from a value of 24% at 350 °C to a minimum of 8% at 600 °C. Both methane and carbon dioxide selectivity increase by increasing the temperature. Although the carbon monoxide selectivity decreases with the temperature, in the best case the product stream cannot be used directly in a fuel cell because of the high CO concentration. Similar results were obtained with the membrane MR2.

Table 3
Lumen and shell gases composition for the MR2

T (°C)	X_{H_2} (%)	X_{CO_2} (%)	X_{CH_4} (%)	X_{CO} (%)
Lumen				
350	54.03	21.98	13.05	10.93
400	52.59	22.90	15.84	8.66
450	55.30	28.31	11.85	4.52
500	54.44	26.25	16.14	3.16
550	54.10	27.70	15.60	2.55
Shell				
350	78.59	6.53	3.21	11.65
400	72.12	11.40	9.60	6.87
450	70.94	12.31	11.31	5.42
500	68.69	16.93	11.42	2.95
550	71.97	16.14	9.06	2.81

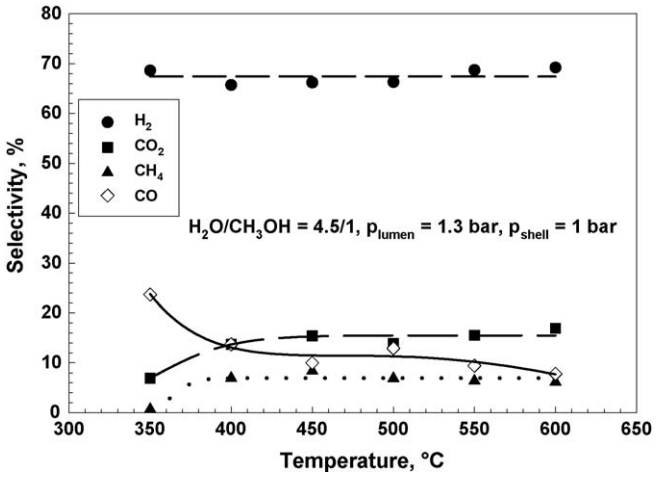

Fig. 3. Different gas selectivities vs. temperature for the MR1, H_2O/CH_3OH = 4.5/1, p_{lumen} = 1.3 bar, p_{shell} = 1 bar.

Fig. 4 shows the hydrogen production as well as the hydrogen lumen and shell flow rates versus temperature for the MR1. It can be seen that, for both shell side and lumen side, the hydrogen flow rate increases by increasing the temperature and these results in the hydrogen production increase with temperature. Also for the membrane MR2 a similar trend is observed. In Fig. 5, the total hydrogen flow rate in the MRs and TR is reported. For temperature higher than 450 °C, the MR1 gives an hydrogen production higher than the TR at the same experimental conditions. For MR2 the hydrogen production increases with the temperature but it is always lower than the hydrogen production in the TR. For MR3 the hydrogen flow rate is always higher than in the other reactors at the same temperature. The hydrogen production strongly increases with the temperature. At 400 °C the hydrogen production in the MR3 is higher than the hydrogen production in the TR operated at 550 °C. In this view the MR3 can be used to obtain the same hydrogen production via methanol steam reforming of a TR but at lower temperature.

Regarding the other gases, Table 4 shows the comparison in terms of gas reaction selectivity for TR, MR1 and MR2. It can

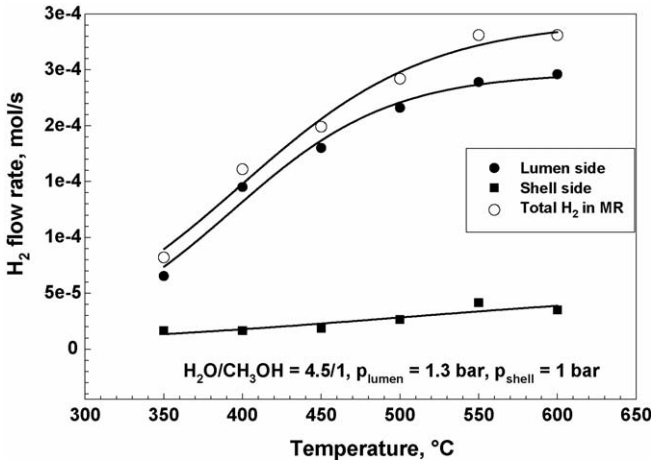

Fig. 4. Hydrogen flow rate vs. temperature for the MR1, H_2O/CH_3OH = 4.5/1, p_{lumen} = 1.3 bar, p_{shell} = 1 bar.

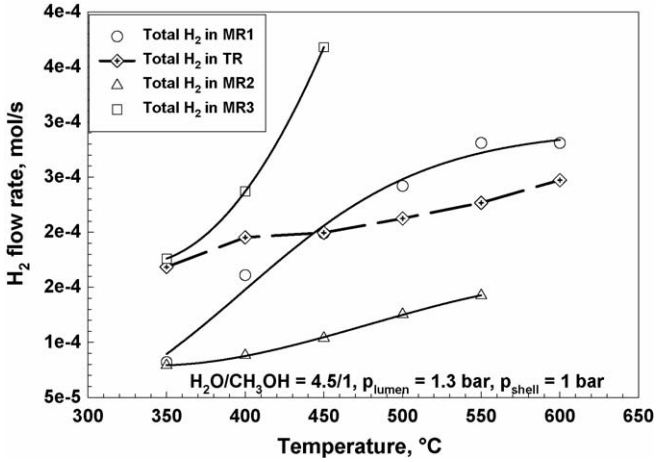

Fig. 5. Hydrogen flow rate vs. temperature for the TR, and the MRs, $H_2O/CH_3OH = 4.5/1$, $p_{lumen} = 1.3$ bar, $p_{shell} = 1$ bar.

be seen that there is a big difference in the product distributions between the TR and the MR1. The most interesting result is that at 600 °C, where the biggest hydrogen production in the MR1 is achieved and, at the same time, the CO content in the stream is lower than the TR at the same experimental conditions. Regarding the MR2, the same table shows that, although the hydrogen selectivity is lower than the TR and the MR1, the CO selectivity, at the maximum temperature, is much lower than the TR and the MR1.

In order to close the holes and so to increase the permselectivities of the MR1 and the MR2 and thus the performances of these membranes towards the methanol steam reforming reaction, other Pd–Ag depositions are necessary.

For these two membranes the sweep gas was not used in order to avoid the back diffusion of this gas in the reaction side of the reactor. For this reason the different sweep gas configurations were not considered.

3.3. Co-current and counter-current modes

For the dense Pd–Ag membrane MR3, which presented the best performances among the three reactors, more experimental tests were performed by using different sweep gas configurations, in fact, both co-current and counter-current modes were considered. The maximum temperature investigated for this membrane was 450 °C. The nitrogen sweep gas flow rate range was 0.5–12 ml/s.

Table 5
Methanol conversion vs. temperature and vs. sweep gas flow rate for the MR3 co-current and counter-current mode

$Q_{sweep-gas}$ (ml/s)	Co-current mode			Counter-current mode		
	350 °C	400 °C	450 °C	350 °C	400 °C	450 °C
	Methanol conversion					
0.501	83%	98%	98%	83%	100%	100%
1.539	84%	99%	99%	84%	100%	100%
3.663	86%	99%	99%	86%	100%	100%
5.961	86%	99%	99%	86%	100%	100%
8.677	87%	100%	100%	87%	100%	100%
11.834	87%	100%	100%	87%	100%	100%

Table 5 summarises the methanol conversion for the MR3 at different sweep gas flow rates and in the two different flow configurations. As already seen for the MR1 and the MR2, the methanol conversion increases with increasing the temperature. For this membrane, the methanol conversion increases also with the sweep gas flow rate and this fact is due to the increase in hydrogen permeation through the membrane with consequent equilibrium shift towards the products. In fact, high sweep gas flow rate means low hydrogen partial pressure in the shell side and, because of Eq. (1), the hydrogen permeation flux increases.

The counter-current mode gives a methanol conversion slightly higher than the co-current mode and this is due to the different hydrogen partial pressure profiles along the reactor in the two configurations.

In the co-current mode, along the axial axis of the reactor the hydrogen partial pressure in the lumen is always higher than the hydrogen partial pressure in the shell side: there is always a driving force higher than zero for the hydrogen permeation. In this way, with a membrane reactor, it is not possible to recover in the permeation zone all the hydrogen produced in the reaction zone, because the hydrogen permeation will stop when the hydrogen partial pressure in the lumen is equal to the hydrogen partial pressure in the shell side. In order to decrease the partial pressure in the shell side, it is possible to use a very large sweep gas flow rate. However, this solution has an economic limitation owing to the cost of the sweep gas and the cost of the separation between the sweep gas and the hydrogen produced, and also a technological limitation owing to the high pressure drop in the shell side of the reactor. Anyway, it should be said that this is only a laboratory solution for reducing the H_2 partial

Table 4
Different gas selectivities vs. temperature for the TR, the MR1 and the MR2

T (°C)	TR				MR1				MR2			
	S_{H_2} (%)	S_{CO_2} (%)	S_{CH_4} (%)	S_{CO} (%)	S_{H_2} (%)	S_{CO_2} (%)	S_{CH_4} (%)	S_{CO} (%)	S_{H_2} (%)	S_{CO_2} (%)	S_{CH_4} (%)	S_{CO} (%)
350	60.25	20.34	14.44	4.97	68.60	6.91	0.68	23.70	61.11	17.53	10.22	11.14
400	61.11	22.43	14.22	2.24	65.70	13.70	6.91	13.70	58.34	19.52	14.01	8.13
450	63.87	21.96	11.56	2.60	66.20	15.40	8.34	10.00	59.73	23.80	11.70	4.78
500	65.26	21.28	9.71	3.75	66.30	13.90	6.88	12.90	58.10	23.86	14.93	3.11
550	65.81	19.38	8.19	6.62	68.70	15.50	6.37	9.41	59.18	24.44	13.75	2.62
600	68.99	18.60	3.90	8.52	69.20	16.90	6.13	7.79	–	–	–	–

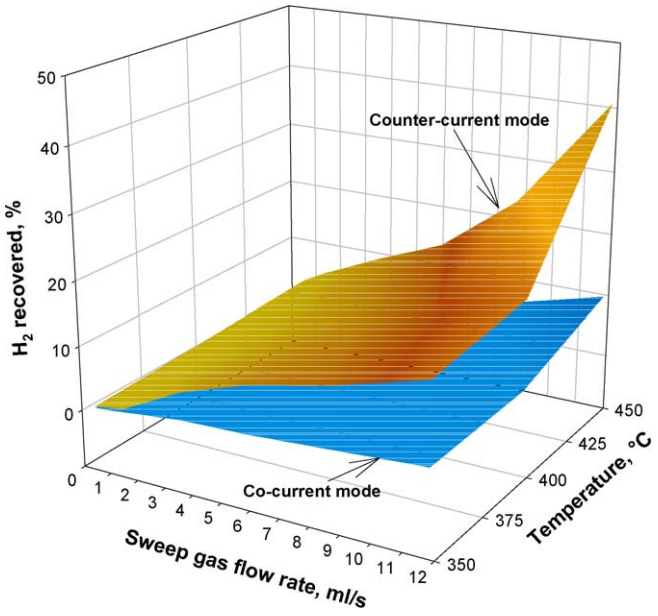

Fig. 6. Hydrogen recovery vs. sweep gas flow rate and vs. temperature for the MR3, H_2O/CH_3OH = 4.5/1, p_{lumen} = 1.3 bar, p_{shell} = 1 bar.

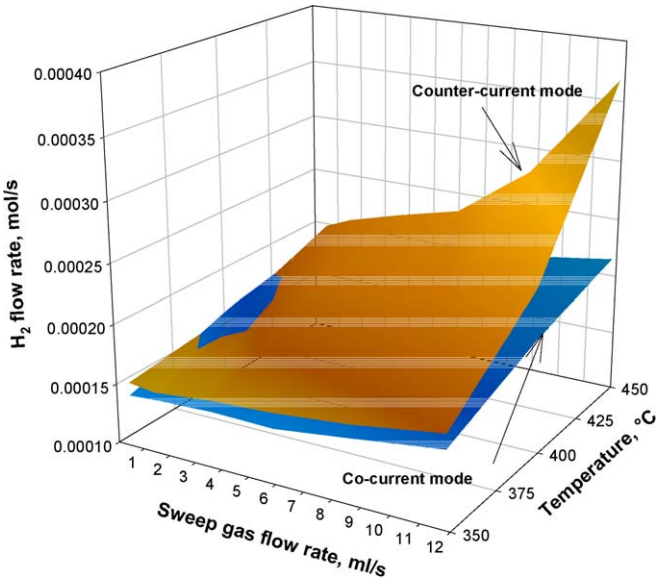

Fig. 7. Hydrogen flow rate vs. sweep gas flow rate and vs. temperature for the MR3, H_2O/CH_3OH = 4.5/1, p_{lumen} = 1.3 bar, p_{shell} = 1 bar.

pressure in shell side: practically, in industrial applications other solutions could be adopted, such as vacuum in the shell side, for example.

This problem can be overcome by using the counter-current mode. In this case the retentate outlet stream corresponds to the permeate inlet stream in which the hydrogen partial pressure is zero. In this case, the outlet permeate hydrogen partial pressure can be almost zero (i.e. by using a very thin membrane thickness or a very large membrane area). This means that in counter-current mode almost all the hydrogen produced in the reaction zone can be recovered in the permeation zone. For this reason, in the counter-current mode the hydrogen recovery is higher than in the co-current mode as shown in Fig. 6. The figure shows that the MR3 in counter-current mode gives a higher hydrogen recovery than the MR3 in co-current mode. In particular, for the co-current mode, the hydrogen recovery is almost 1% at low sweep gas flow rate and low temperature and is maximum (10%) at high sweep gas flow rate and high temperature. The counter-current mode presents the same trend of the co-current mode but the hydrogen recovery is always higher than the last one. In particular, the maximum hydrogen recovery is 40% at high sweep gas flow rate and high temperature (against 10% for co-current). At low temperature and low sweep gas flow rate, the difference between co-current and counter-current is so low that, practically, it cannot be distinguished from the experimental error.

In Fig. 7, the total hydrogen production (lumen side + shell side) against the temperature and the sweep gas flow rate is reported. Also in this case, the trend is the same as the previous figure with a big difference in the hydrogen production between co-current and counter-current mode at high sweep gas flow rate and high temperature.

Table 6 shows a comparison between the TR, the MR1 and the MR3 in terms of total hydrogen production versus temperature. It can be seen that the MR3 in counter-current mode gives the best result compared with the other reactors, even better than the TR operated at temperature 150 °C higher than the MR3.

This comparison shows that the dense Pd–Ag membrane reactor gives higher conversion and higher total hydrogen production than the other reactors but, the most important result is that in this reactor a CO-free hydrogen stream is available to feed directly a PEM fuel-cell system. In counter-current mode this hydrogen stream is 40% of the total hydrogen produced in the reactor.

To the best of our knowledge, no paper dealing with MSR by using $Ru–Al_2O_3$ catalyst is presented in the literature, so a direct comparison is not possible. A comparison is possible for the Pd–Ag dense membrane, because the same membrane was used for the same reaction in a previous work [21]. In that work a Cu-based commercial catalyst was used to carry out the MSR. A comparison is reported in Fig. 8 which shows the methanol conversion versus temperature for the MSR with Cu-based catalyst, the oxidative MSR with Cu-based catalyst and the MSR with Ru-based catalyst. In each case the dense Pd–Ag

Table 6
Hydrogen production vs. temperature for the TR, the MR1, the MR3 co-current and counter-current mode

$Q_{H_2\text{-TOT}}$ (mol/s)				
T (°C)	TR	MR1	MR3 co-current	MR3 counter-current
350	1.68E−04	8.20E−05	1.64E−04	1.76E−04
400	1.95E−04	1.61E−04	1.94E−04	2.37E−04
450	1.99E−04	1.99E−04	2.15E−04	3.68E−04
500	2.12E−04	2.42E−04		
550	2.27E−04	2.81E−04		
600	2.47E−04	2.81E−04		

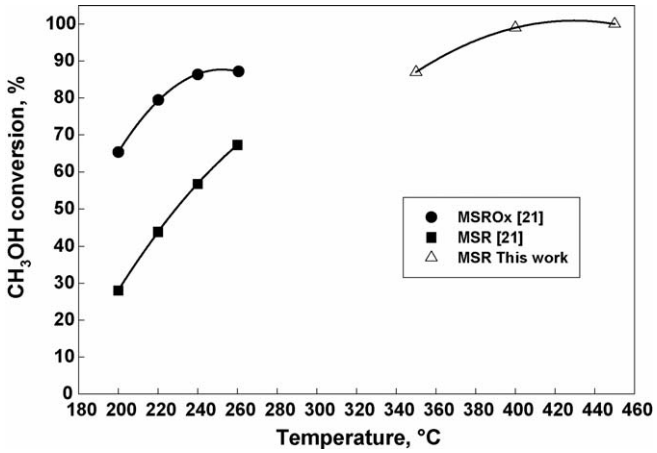

Fig. 8. Methanol conversion vs. temperature for the MR3 and literature data.

membrane reactor showed higher performances than the corresponding TR.

In the following we summarise the advantages and the disadvantages in the use of different catalysts in the MR.

The Cu-based catalyst has a maximum operative temperature of 300 °C, after that the catalyst quickly loses its activity because of the Cu particles sintering. For this reason the MSR reaction has to be carry out at temperatures in the range 200–280 °C. In this range, in order to have high methanol conversion and high hydrogen recovery, high pressure and low space velocity (SV) are necessary. The data summarised in Fig. 8 for this catalyst were obtained at SV = $4.5 \times 10^{-4}\,\mathrm{mol_{CH_3OH}}/(\mathrm{min\,g_{cat}})$ and lumen side pressure of 2.6 bar and sweep gas flow rate 0.31 ml/s. In order to increase the methanol conversion, oxygen can be added to the feed resulting in the oxidative MSR reaction. In this case the methanol conversion increases both at a fixed temperature and with increasing the temperature. In each case, the main problem is the formation of carbon deposit on the catalyst surface which results in a steady state activity for 5 h and afterwards a loss in the catalytic activity. The re-activation of the catalyst could result in high temperature and hot-spot on the catalytic surface. The problem can be just solved by working at low temperature, low oxygen content and high H_2O/CH_3OH feed ratio.

For the Ru-based catalyst the operative temperature has to be higher than the Cu-based catalyst, and this is the disadvantage. The advantages are that the conversion is much higher (almost 100%) also by operating at lower pressure (1.3 bar) and higher SV ($2.5 \times 10^{-2}\,\mathrm{mol_{CH_3OH}}/(\mathrm{min\,g_{cat}})$). The high conversion at higher SV gives an idea of the higher activity of the Ru-based catalyst than the Cu-based one. The sweep gas flow rate (0.5 ml/s) is almost the same as the reactor with Cu-based catalyst. The most important result is that no deactivation was observed during the experiments. Moreover, the catalytic activity was constant during the experimental tests up to 20 h.

All the experimental results reported in the present work are average values of different experimental points (at least 3). The balance on the C is closed with a ±5% error.

4. Conclusions

The methanol steam reforming reaction has been studied from an experimental point of view in a TR and in different MRs. Two Pd–Ag supported membranes (MR1 and MR2) and a dense Pd–Ag membrane (MR3) were used in order to increase the methanol conversion and the hydrogen production. The first membrane was able to increase the methanol conversion and the hydrogen production as well as to decrease the carbon monoxide selectivity with respect to the TR. The second membrane is not able to improve the performances of a TR, just the carbon monoxide selectivity is lower than the TR at high temperature. The third membrane (Pd–Ag dense membrane) is able to give: (a) high methanol conversion; (b) high hydrogen production; (c) low carbon monoxide selectivity. The best results with this membrane are obtained by operating the reactor in counter-current mode at high temperature and high sweep gas flow rate, when 40% of the total hydrogen produced is recovered as a CO-free hydrogen stream. Furthermore, both the manufacturing procedure and the finger-type configuration assure a long life of the Pd–Ag membrane as well as infinite hydrogen selectivity. The present work shows, for a dense Pd–Ag membrane, how it is possible to improve the membrane reactor performances by using the counter-current mode instead of the co-current mode, when all the other operative parameters are kept constant. To optimise the hydrogen recovery in the counter-current mode a higher reaction pressure can be used in a future work.

References

[1] P.J. de Wild, M.J.F.M. Verhaak, Catalytic production of hydrogen from methanol, Catal. Today 60 (2000) 3–10.
[2] W. Wiese, B. Emonts, R. Peters, Methanol steam reforming in a fuel cell drive system, J. Power Sources 84 (1999) 187–193.
[3] J.P. Breen, R. Burch, H.M. Coleman, Metal-catalysed steam reforming of ethanol in the production of hydrogen for fuel cell applications, Appl. Catal. B: Environ. 39 (2002) 65–74.
[4] S. Cavallaro, V. Chiodo, A. Vita, S. Freni, Hydrogen production by auto thermal reforming of ethanol on Rh–Al_2O_3 catalyst, J. Power Sources 123 (2003) 10–16.
[5] G. Maggio, S. Freni, S. Cavallaro, Light alcohols/methane fuelled molten carbonate fuel cells: a comparative study, J. Power Sources 74 (1998) 17–23.
[6] A. Heinzel, B. Vogel, P. Hubner, Reforming of natural gas-hydrogen generation for small scale stationary fuel cell systems, J. Power Sources 105 (2002) 202–207.
[7] J.-P. Shen, C. Song, Influence of preparation method performance of Cu/Zn-based catalysts for low-temperature steam reforming and oxidative steam reforming of methanol for H_2 production for fuel cells, Catal. Today 77 (2002) 89–98.
[8] B. Lindstrom, L.J. Pettersson, Hydrogen generation by steam reforming of methanol over copper-based catalysts for fuel cell applications, Int. J. Hydrogen Energy 26 (2001) 923–933.
[9] J. Han, I.S. Kim, K.S. Choi, Purifier-integrated methanol reformer for fuel cell vehicles, J. Power Sources 86 (2000) 223–227.
[10] Y.M. Lin, M.H. Rei, Study on the hydrogen production from methanol steam reforming in supported palladium membrane reactor, Catal. Today 67 (2001) 77–84.
[11] B. Emonts, J.B. Hansen, H. Schmidt, T. Grube, B. Höhlein, R. Peters, A. Tschauder, Fuel cell drive system with hydrogen generation in test, J. Power Sources 86 (1/2) (2000) 228–236.
[12] S. Wieland, T. Melin, A. Lamm, Membrane reactors for hydrogen production, Chem. Eng. Sci. 57 (9) (2002) 1571–1576.

[13] Y.M. Lin, M.H. Rei, Process development for generating high purity hydrogen by using supported palladium membrane reactor as steam reformer, Int. J. Hydrogen Energy 25 (2000) 211–219.
[14] K. Sekizawa, S. Yano, K. Eguchi, H. Arai, Selective removal of CO in methanol reformed gas over Cu-supported mixed metal oxides, Appl. Catal. A: Gen. 169 (1998) 291–297.
[15] T. Takahashi, M. Inoue, T. Kai, Effect of metal composition on hydrogen selectivity in steam reforming of methanol over catalysts prepared from amorphous alloys, Appl. Catal. A: Gen. 218 (2001) 189–195.
[16] J. Agrell, H. Birgersson, M. Boutonnet, Steam reforming of methanol over a $Cu/ZnO/Al_2O_3$ catalyst: a kinetic analysis and strategies for suppression of CO formation, J. Power Sources 106 (1/2) (2002) 249–257.
[17] J.C. Amphlett, M.J. Evans, R.A. Jones, R.F. Mann, R.D. Weir, Hydrogen production by the catalytic steam reforming of methanol. Part 1. The thermodynamics, Can. J. Chem. Eng. 59 (1981) 720–727.
[18] F. Gallucci, L. Paturzo, A. Basile, Hydrogen recovery from methanol steam reforming in a dense membrane reactor: simulation study, Ind. Eng. Chem. Res. 43 (10) (2004) 2420–2432.
[19] F. Gallucci, A. Basile, Co-current and counter-current modes for methanol steam reforming membrane reactor, Int. J. Hydrogen Energy, submitted for publication.
[20] A. Basile, F. Gallucci, L. Paturzo, A dense Pd/Ag membrane reactor for methanol steam reforming: experimental study, Catal. Today 114 (2005) 244–250.
[21] A. Basile, F. Gallucci, L. Paturzo, Hydrogen production from methanol by oxidative steam reforming carried out in a membrane reactor, Catal. Today 114 (2005) 251–259.
[22] A. Basile, S. Tosti, Dispositivo portatile a membrana intercambiabile per valutazione di processi di permeazione e reazione in fase gassosa, Italian Patent Application RM2005U000107.
[23] S. Tosti, L. Bettinali, Diffusion bonding of Pd–Ag membranes, J. Mater. Sci. 39 (2004) 3041–3046.
[24] S. Tosti, L. Bettinali, D. Lecci, F. Marini, V. Violante, Method of bonding thin foils made of metal alloys selectively permeable to hydrogen, particularly providing membrane devices, and apparatus for carrying out the same, European Patent EP 1184125.
[25] A. Basile, L. Paturzo, F. Laganà, The partial oxidation of methane to syngas in a palladium membrane reactor: simulation and experimental studies, Catal. Today 67 (2001) 65–75.
[26] S.A. Koffler, J.B. Hudson, G.S. Ansell, Hydrogen permeation through alpha-palladium, Trans. AIME 245 (1969) 1735–1740.
[27] Yu.A. Balovnev, Diffusion of hydrogen in palladium'', Russ. J. Phys. Chem. 48 (1974) 409–410.
[28] N. Itoh, W.C. Xu, K. Haraya, Basic experimental study on palladium membrane reactors, J. Membr. Sci. 66 (1992) 149–155.
[29] N. Itoh, W.C. Xu, Selective hydrogenation of phenol to cyclohexanone using palladium-based membranes as catalysts, Appl. Catal. A: Gen. 107 (1993) 83–100.